Local Structure Formation in Alkyl-imidazolium-Based Ionic Liquids as Revealed by Linear and Nonlinear Raman Spectroscopy

KOICHI IWATA,[†] HAJIME OKAJIMA,[‡] SATYEN SAHA,[§] AND HIRO-O HAMAGUCHI*[,‡,||]

Research Centre for Spectrochemistry and Department of Chemistry, School of Science, The University of Tokyo, 7-3-1 Hongo, Bunkyo-ku, Tokyo 113-0033, Japan, Department of Chemistry, Banaras Hindu University; Varanasi 221005, India, and Institute of Molecular Science and Department of Applied Chemistry, National Chiao Tung University; 1001 Ta Hsueh Road, Hsinchu 300, Taiwan

Received May 21, 2007

ABSTRACT

We show several pieces of Raman spectroscopic evidence that are indicative of local structure formation in imidazolium-based ionic liquids. Low-frequency Raman spectra of $C_n$mimX, where $C_n$mim stands for 1-alkyl(C_nH_{2n+1})-3-methylimidazolium cation and X represents the anion, exhibit broad bands assignable to collective modes of local structures. Spatial distributions of coherent anti-Stokes Raman scattering (CARS) signals from $C_n$mim[PF_6] are consistent with local structures whose size increases with increasing *n*. Picosecond Raman spectra of S_1 *trans*-stilbene as a "picosecond Raman thermometer" show microscopic thermal inhomogeneity ascribable to local structure formation in C_2mimTf_2N and C_4mimTf_2N. We also describe two novel phenomena that we believe are relevant to extraordinary nanoenvironments generated by local structures in a magnetic ionic liquid C_4mim[$FeCl_4$].

Introduction

Liquids are much less understood than gases and crystals. The structure of molecules in the gas phase can be accurately determined by electron diffraction or high-resolution rotationally resolved spectroscopy. Molecular structures and their three-dimensional arrangements in crystals can be determined by X-ray or neutron diffraction. The diffraction and spectroscopic methods are also applicable to liquids, but with only limited resolution. Diffraction patterns become diffuse and rotational structures lost in the liquid phase. Structural information available for liquids is thus dilute. Molecules are disordered in gases, but they are ordered in crystals. What happens in liquids?

Recent research focus on ionic liquids is casting a new light upon this problem.[1] Ionic liquids are composed solely of ions. Unlike ordinary molecular liquids, Coulomb interaction may play a major role in these liquids. The long-range nature of Coulomb interaction may give rise to structure and dynamics that are unique to ionic liquids but are not associated with molecular liquids. The many novel features of ionic liquids are likely to originate from these unique structures and dynamics. Ionic liquids are extreme examples of liquids that are highly informative and suitable for investigating possible molecular orderings in liquids.

Raman spectroscopy provides vibrational Raman spectra that are often called "molecular fingerprints". From these fingerprints, we are able to learn in detail the structure and dynamics of molecules (ions). The versatility of Raman spectroscopy enables us to measure Raman spectra and hence comparatively study molecules in different phases or states. In fact, we found the rotational isomerism in 1-butyl-3-methyl-imidazolium (C_4mim)-based ionic liquids[2] by comparing the Raman spectra of supercooled liquid C_4mimCl and those of the two polymorphs of crystalline C_4mimCl, for which crystal and molecular structures are solved.[3–5] In $C_n$mim-based ionic liquids, at least two rotational isomers of the $C_n$mim cation coexist, one with a trans and the other with a gauche conformation with respect to the C_7–C_8 bond of the alkyl group, where C_7 is the second carbon atom of the alkyl group attached to the imidazolium ring.[1] The trans isomer is more stable than the gauche as is the case in nonpolar organic molecular liquids. However, the measured enthalpy differences in $C_n$mim[BF_4] (n = 3–10)[1] are much smaller than the common value for neat alkane liquids at room temperature.[6,7] It has also been found that the enthalpy difference increases with increasing the chain length *n*. These findings indicate that the alkyl chains in liquid $C_n$mim[BF_4] are not free to change conformation but are subject to strong intermolecular interactions and that these interactions become stronger in longer alkyl chains. Based on these Raman spectroscopic implications,

Koichi Iwata received a B.Sc. (University of Tokyo, 1984), M.Sc. (University of Tokyo, 1986), and D.Sc. (University of Tokyo,1989) and was a Postdoctoral Fellow at The Ohio State University (1989), a Research Associate at Kanagawa Academy of Science and Technology (1991), a Visiting Research Associate Professor at Waseda University (1997), and an Associate Professor at University of Tokyo, 1997 with research interests in physical chemistry and time-resolved spectroscopy.

Hajime Okajima received a B.Sc. (University of Tokyo, 2005) and M.Sc. (University of Tokyo, 2007) and is currently a JSPS research fellow (2007) with research interests in molecular spectroscopy and structural chemistry.

Satyen Saha received a B.Sc. (Jadavpur University, 1994), M.Sc. (Jadavpur University, 1996), and Ph.D. (Hyderabad Central University, 2002) and was a Postdoctoral researcher at University of Tokyo (2002–2005) and a Lecturer at Banaras Hindu University (2006) with research interests in structure and dynamics of ionic liquids and fluorescent molecules in condensed phases.

[†] Research Centre for Spectrochemistry, School of Science, The University of Tokyo.

[‡] Department of Chemistry, School of Science, The University of Tokyo.

[§] Banaras Hindu University.

[||] National Chiao Tung University.

Hiro-o Hamaguchi received a B.Sc. (University of Tokyo, 1970), M.Sc. (University of Tokyo, 1972), and D.Sc. (University of Tokyo, 1975) and was a Research Associate at University of Tokyo (1975), a Lecturer at University of Tokyo (1981), an Associate Professor at University of Tokyo (1983), a Laboratory Head at Kanagawa Academy of Science and Technology (1990), a Professor at University of Tokyo (1995), President of the Spectroscopical Society of Japan (2003–2005), and Chair Professor at National Chiao Tung University, Taiwan (2007) with research interests in molecular spectroscopy, structural chemistry, photomolecular science, and biophysical chemistry.

10.1021/ar700074c CCC: $37.00
Published on Web 10/27/2007

together with a wide-angle X-ray diffraction result,[8] we have built a working hypothesis that these ionic liquids are not homogeneous at the microscopic level but that they form specific local structures.[1] The possibility of local structure formation in ionic liquids has been discussed from various viewpoints: X-ray diffraction,[9,10] diffusion measurement,[11,12] neutron diffraction,[13] ultrafast photoexcited dynamics,[14–18] and molecular dynamics simulations.[19–22]

In the present Account, we discuss our recent Raman spectroscopic results that further support our working hypothesis. Low-frequency Raman spectra of liquid $C_n$mim[PF_6] ($n = 4, 6, 8$) are shown to exhibit broad features assignable to collective modes of local structures with different size. Spatial distributions of coherent anti-Stokes Raman scattering (CARS) signals from $C_n$mim[PF_6] show characteristic broadening ascribed to local structures whose average size is larger for larger *n*. Picosecond time-resolved Raman results are discussed with a focus placed on the cooling process of photoexcited *trans*-stilbene in C_2mimTf_2N and C_4mimTf_2N. The observed cooling rates are not correlated with macroscopic thermal diffusivity, contrary to what we observed for molecular liquids, suggesting that these ionic liquids are thermally inhomogeneous. Finally, two newly found phenomena are described, which are indicative of extraordinary nanoenvironments in a magnetic ionic liquid, C_4mim[$FeCl_4$]. Though information carried by these experimental results is rather indirect, as is always the case with structural studies of liquids, they all point to the same direction of local structure formation in imidazolium-based ionic liquids.

Low-Frequency Raman Spectra and Collective Cationic Motions in $C_n$mim[PF_6]

In low-frequency Raman spectra of liquids, various collective modes are expected to appear in addition to intramolecular vibrational modes.[23,24] We are able to study those collective modes, which must bear key information for understanding ionic liquid structures, by measuring low-frequency Raman spectra. Though similar information is obtainable with the ultrafast optical Kerr effect (OKE) method[25–32] and also by far-infrared/terahertz spectroscopy,[33,34] Raman spectroscopy is more advantageous for its versatility. It would be difficult to measure by OKE or far-infrared/terahertz spectroscopy both the liquid and solid samples under the same experimental conditions.

A typical Raman spectrum of C_4mim[PF_6] is shown in Figure 1a. A shoulder-like Raman band is observed in the low-frequency region below 100 cm^{-1}. In order to discuss the low-frequency spectra quantitatively, we reduce the observed spectra by the following formula:[35]

$$I_{red}[\tilde{\nu}] = \left(1 - e^{-\frac{ch\tilde{\nu}}{kT}}\right)(\tilde{\nu}_0 - \tilde{\nu})^{-3} I_{obs}[\tilde{\nu}] \qquad (1)$$

Here $\tilde{\nu}_0$ is the wavenumber of Stokes Raman shift, $\tilde{\nu}_0$ is the wavenumber of the incident laser light, *c* is the velocity of light, *k* is the Boltzmann constant, and *T* is the absolute temperature. The resultant reduced spectrum of C_4mim[PF_6] is shown in Figure 1b. The intensities in the reduced spectrum are proportional to the Raman scattering cross sections of the $\nu = 1 \leftarrow \nu = 0$ transitions, where ν is the vibrational quantum number. The physical meaning of reducing a Raman spectrum is to cancel out the effect of thermal excitation and make the spectrum comparable to calculated Raman intensities. Note that the negative feature in the anti-Stokes region in the reduced spectrum is the inverted mirror image of the Stokes region.

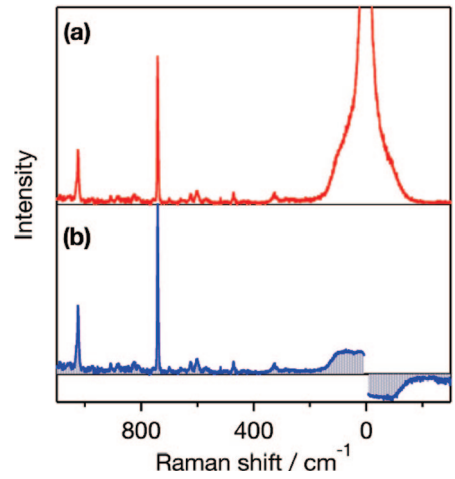

FIGURE 1. The observed (a) and reduced (b) Raman spectra of C_4mim [PF_6].

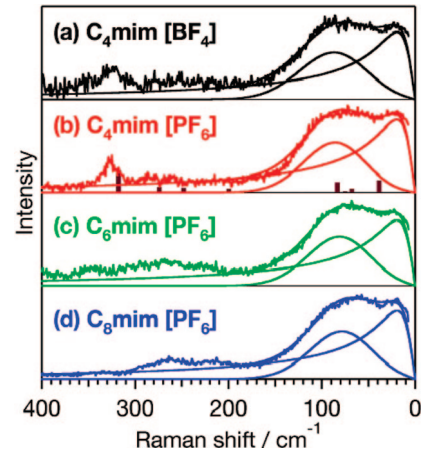

FIGURE 2. Reduced Raman spectra for $C_n$mimX ionic liquids: (a) C_4mim[BF_4]; (b) C_4mim[PF_6]; (c) C_6mim[PF_6]; (d) C_8mim[PF_6]. The solid lines indicate the fitting results. The vertical bars indicate the calculated results for the C_4mim cation.

The reduced Raman spectra of $C_n$mim-based ionic liquids are compared in Figure 2. We compare C_4mim[BF_4] and C_4mim[PF_6] for examining the anion dependence and C_4mim[PF_6], C_6mim[PF_6], and C_8mim[PF_6] for investigating the dependence on the alkyl chain length of the cation. For the sake of quantitative discussion, these spectra are fitted by simple model functions assuming two independent components. One is a Gaussian band that is related to an inhomogeneously broadened vibrational band. The other is a relaxation band that corresponds to a Debye-type relaxational motion. The observed spectra are very well fitted with the model functions corresponding to the two components. The best-fitted curves are shown in Figure 2 by the solid lines. The peak position Ω and the width Γ of the Gaussian component obtained

Table 1. The Peak Position Ω and Width Γ of the Gaussian Component in the Low-Frequency Raman Spectrum of $C_n$mimX

	Ω, cm^{-1}	Γ, cm^{-1}
C_4mim[BF_4]	69 ± 2	40 ± 2
C_4mim[PF_6]	71 ± 2	36 ± 2
C_6mim[PF_6]	64 ± 2	37 ± 2
C_8mim[PF_6]	62 ± 2	37 ± 2

from the best fit are listed in Table 1. The relaxational components have similar widths in all measured ionic liquids. They are around 20 cm^{-1} (corresponding to about 1 ps damping time constant) and correctly reproduce the baselines of the spectra in the 200–600 cm^{-1} region.

The peak position Ω of the Gaussian component shows no appreciable anion dependence, but it deceases systematically with increasing chain length, *n*, of the cation. It is therefore considered that the Gaussian vibrational bands are due to cationic motions. However, these bands are not assignable to intracationic vibrations, because their area intensities are much higher than those of the other intracationic bands. In fact, a quantum chemical calculation of an isolated C_4mim^+ cation at the B3LYP/6-31+G** level[36] predicts only very weak bands around 80 cm^{-1} (vertical bars in Figure 2b). We therefore assign these Gaussian components to inhomogeneously broadened bands due to collective motions of cations involved in local structures. We note that a similar band in an OKE spectrum has been assigned to a librational mode.[26] The unusually large widths, 35–40 cm^{-1}, are consistent with local structures having different size.

In the 200–400 cm^{-1} region, we observe a few bands assignable to intracationic modes. It is known that the accordion vibration of alkyl chain (in-phase C–C–C bend) exists in this frequency region.[37] According to the quantum chemical calculation, the 330 cm^{-1} band of C_4mim[PF_6] is assignable to the accordion vibration from the butyl chain, coupled with the out-of-plane vibration of the imidazolium cation. If the chain length of the cation becomes longer, the frequency of the accordion vibration shifts to lower frequency. Corresponding to this expectation, we find broad features in the 200–300 cm^{-1} region of the spectra of C_6mim[PF_6] and C_8mim[PF_6]. It seems that the accordion band becomes broader as well with increasing *n*. This observation is consistent with stronger interchain interactions in liquid $C_n$mim[PF_6] with larger *n*. The peak position Ω of the Gaussian component and the width of the accordion band both change more markedly between $n = 4$ and $n = 6$ than between $n = 6$ and $n = 8$. It seems that the liquid structure changes more on going from C_4mim[PF_6] to C_6mim[PF_6] than from C_6mim[PF_6] to C_8mim[PF_6].

Local Structures in $C_n$mim[PF_6] as Revealed by Spatial Distribution of Coherent Anti-Stokes Raman Scattering (CARS)

It has recently been shown by us that the local structures in liquids and solutions can be sensitively probed by measuring the spatial distribution of coherent anti-Stokes Raman scattering (CARS) signals.[38,39] In CARS, two laser beams with ω_1 and ω_2 angular frequencies and with $\mathbf{k}_1$ and $\mathbf{k}_2$ wavenumber vectors, respectively, are incident on a sample medium. If the frequency difference $\omega_1 - \omega_2$ coincides with the frequency Ω of a Raman active transition ($\omega_1 - \omega_2 = \Omega$, Raman resonance), a coherent CARS signal is emitted in the phase-matched direction determined as $2\mathbf{k}_1 - \mathbf{k}_2 = \mathbf{k}$ (Figure 3). This phase-matching condition is derived on the assumption that the interaction length *L* of the incident radiations with the medium is much larger than their wavelengths, λ_1 and λ_2 ($L \gg \lambda_1$ and λ_2). In other words, the sample medium must be optically homogeneous (invariant refractive index) over a range much larger than λ_1 and λ_2. In reality, however, the sample medium can be optically inhomogeneous (distributed refractive index) for many reasons. If, for example, the sample liquid has mesoscopic local structures, the refractive index of the medium varies microscopically, even though it is transparent and seemingly homogeneous, and the interaction length *L* is limited due to this optical inhomogeneity. Then, the phase-matching condition is relaxed and a portion of CARS signal is emitted off from the phase-matched direction ($\theta > 0$ in Figure 3). This phase-mismatched CARS signal at $\theta = 90°$ was already measured and studied as partially coherent anti-Stokes Raman scattering (PCARS).[40,41] The correlation of the PCARS intensities with the optical inhomogeneity in binary liquid mixtures was discussed with reference to Rayleigh scattering intensities.[41] If the spatial distribution of the phase-mismatched CARS signal is measured as a function of θ, it gives more-detailed information on the optical inhomogeneity in the medium. We recently used polystyrene beads of different size (100 and 350 nm in diameter) dispersed in water as a model system and quantitatively examined the CARS signal spatial distribution.[38] The CARS signal from the ring breathing vibration of polystyrene was measured as a function of θ. The observed spatial distribution showed clear dependence on the bead size, with larger beads giving less broadened distribution. This size dependence was successfully reproduced by a theoretical simulation assuming a microscopic distribution of refractive index that corresponds to random location of polystyrene spheres in water.[38] Thus, measurement of the CARS signal spatial distribution has been shown to provide quantitative information on the size or extent of the optical inhomogeneities existing in liquids.

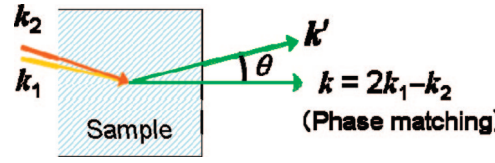

FIGURE 3. Phase matching condition and spatial distribution of CARS signal.

If local structures are formed in ionic liquids, they give rise to optical inhomegeneities, and they can be probed by CARS. Figure 4 shows the measured CARS signal spatial distributions of the totally symmetric PF stretch mode of PF_6^- in liquid C_4mim[PF_6], C_6mim[PF_6], and C_8mim[PF_6].[39] The spatial distribution becomes narrower on going from C_4mim[PF_6] to C_8mim[PF_6], unequivocally

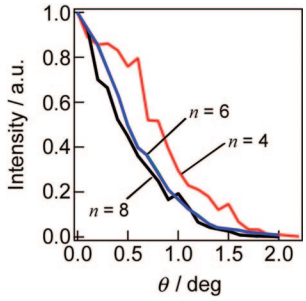

FIGURE 4. Spatial distribution curves of the CARS intensities of the totally symmetric PF stretch mode of PF_6^- in C_4mim[PF_6] (red), C_6mim[PF_6] (blue), and C_8mim[PF_6] (black).

indicating that these three ionic liquids are optically inhomogeneous at the microscopic level and generate significant phase-mismatched CARS signals. It also indicates that the inhomogeneity is less extensive in C_4mim[PF_6] than in C_6mim[PF_6] and C_8mim[PF_6]. In other words, there exist local structures giving rise to optical inhomogeneity, and these local structures are more extensive in ionic liquids with longer alkyl chains. Since we are looking at the CARS signal from the PF_6^- anion, only the inhomogeneities in the anion distribution are detected, but they must be accompanied with the inhomogeneities of the cation distribution. More extensive local structures in $C_n$mim[PF_6] with larger n are consistent with the results discussed in the preceding section, since stronger interactions in longer alkyl chains are likely to generate local structures with larger size. Furthermore, the trend gives plausible explanation to the fact that the shear viscosity increases rapidly with increasing n: C_4mim[PF_6], 371 cP; C_6mim[PF_6], 680 cP; C_8mim[PF_6], 866 cP.[42] Here again, we see that changes are larger on going from $n = 4$ to $n = 6$ than on going from $n = 6$ to $n = 8$.

The size of the detected local structures of $C_n$mim[PF_6] is not clear yet. It is certain that the size is smaller than the wavelength of visible light, because they are all transparent. Considering the fact that the polystyrene beads with 100 nm radius give similar width of CARS spatial distribution as that of C_4mim[PF_6], we can estimate that the size of local structures ranges between a few tens of nanometers and a few hundred nanometers. However, this estimation needs to be refined by comparison of the experimental spatial distribution with theory, in particular, with molecular dynamics simulations. We note that recent molecular dynamics simulation[20,21] and X-ray[10] studies have suggested much smaller size (a few to several nanometers) of local structures.

Microscopic Energy Transfer and Local Structures in Ionic Liquids Probed with a "Picosecond Raman Thermometer"

Energy transfer is a fundamental process in the condensed phase, in which a molecule exchanges its energy with the surrounding molecules constantly through intermolecular interactions. Monitoring the energy transfer process therefore gives quantitative information about the intermolecular interactions in the condensed phase. One of the most effective ways for studying energy transfer is to record the cooling kinetics of a probe molecule after instantaneous excitation of its vibrational states. Immediately after the excitation, the probe molecule starts cooling toward the thermal equilibrium by transferring the excess vibrational energy to the surrounding molecules. Because this vibrational cooling proceeds in a few picoseconds to a few hundreds of picoseconds,[43] time-resolved spectroscopy with time resolution of a few picoseconds is required. More than a decade ago, we constructed a transform-limited picosecond time-resolved Raman spectrometer[44] and started studying picosecond vibrational dynamics of molecules in liquids and solutions.[45] In the course of these studies, we found that the C=C stretch Raman band of the first excited singlet (S_1) state of *trans*-stilbene (*t*SB)[46–49] showed linear dependence on temperature and that it served as an excellent "picosecond Raman thermometer".[49] Recently, we have examined the cooling kinetics of S_1 *t*SB in ionic liquids by using this picosecond Raman thermometer.[50]

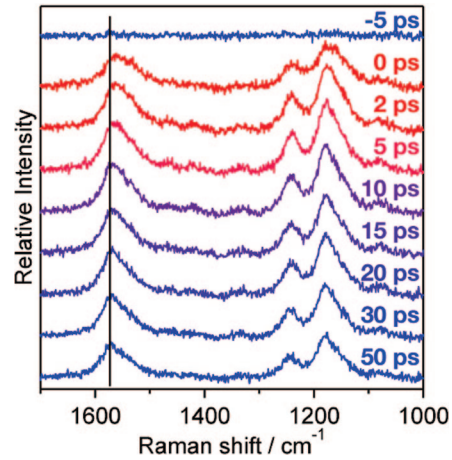

FIGURE 5. Time-resolved Raman spectra of S_1 *trans*-stilbene in C_2mimTf_2N.

We measure picosecond time-resolved Raman spectra with the pump–probe method. The stilbene molecule is photoexcited to the S_1 state with the pump pulse at 296 nm. The produced S_1 state is monitored with the probe pulse at 592 nm, which is in resonance with the S_n–S_1 absorption. With this setting of the pumping wavelength, an excess energy of 3000 cm^{-1} is deposited to S_1 *t*SB. Time resolution of the spectrometer, estimated by the cross-correlation function between the pump and probe pulses, is 1.7 ps.

A set of time-resolved Raman spectra of S_1 *t*SB measured in a C_2mimTf_2N solution (5.0×10^{-3} mol·dm^{-3}) is shown in Figure 5.[50] The Raman bands from the solvent C_2mimTf_2N have been subtracted in the spectra. It is clear from the figure that the C=C stretch band near 1570 cm^{-1} shifts toward higher wavenumbers with increasing time delay. This shift reflects the temperature decrease of the S_1 *t*SB molecule during the cooling process.[49] The cooling curve of S_1 *t*SB, obtained by plotting the peak position of the 1570 cm^{-1} band against the time delay, is fitted well with a single exponential function. The obtained rate constants are summarized in Table 2.

Table 2. Vibrational Cooling Rates (k_{vib}) of S_1 *t*SB and Thermal Diffusivity (κ) of the Solvent

solvent	k_{vib}, ps^{-1}	κ, 10^{-8} m^2 s^{-1}
C_2mimTf_2N	0.11 ± 0.02	6.01 ± 0.04[b]
C_4mimTf_2N	0.12 ± 0.02	6.0 ± 0.1[b]
heptane	0.08[a]	8.01[a]
ethanol	0.13[a]	8.70[a]

[a] Reference 45. [b] Reference 47.

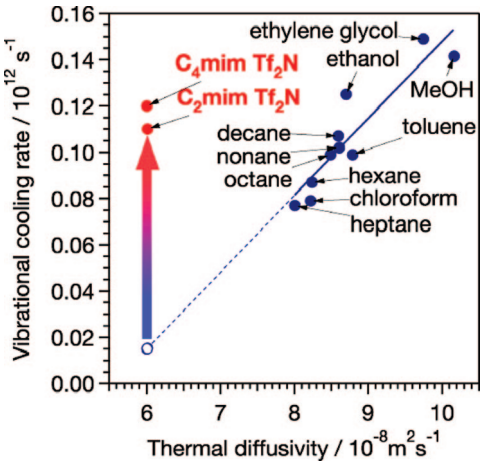

FIGURE 6. Vibrational cooling rate of S_1 *trans*-stilbene and thermal diffusivity of solvent. The solid line represents the correlation between the vibrational cooling rate and thermal diffusivity observed in molecular liquids, whereas the dotted portion indicates the extrapolated values.

We previously measured similar cooling kinetics of S_1 *t*SB in ten molecular liquids.[49] The obtained rate constants showed a good correlation with the thermal diffusivity κ of the solvent. Thermal diffusivity characterizes the macroscopic heat conduction in the solvent, which is well represented by the diffusion equation of heat:

$$\frac{\partial U}{\partial t} = \kappa \Delta U \qquad (2)$$

Here, U is temperature and t is time. The diffusion equation of heat is directly derived from the continuity equation and Fourier's law of heat conduction. Figure 6 shows the plot of the observed cooling rate of S_1 *t*SB vs thermal diffusivity in ten molecular liquids and two ionic liquids. A clear relation between the cooling rate and the thermal diffusivity is observed for the molecular liquids. We have explained this observation by assuming the following scheme of thermal energy transfer. The excess energy first given to S_1 *t*SB is shared in the first solvation shell within the time resolution of the experiment (a few picoseconds). The solvent–solvent energy transfer then follows. The whole cooling rate is controlled by the heat transfer process in the solvent, which is characterized well by thermal diffusivity. The cooling rates observed in the ionic liquids are, however, not explainable by the simple model that we proposed for molecular liquids. The reported values of thermal diffusivity[51] for C_2mimTf_2N and C_4mimTf_2N, $(6.01 \pm 0.04) \times 10^{-8}$ m^2 s^{-1} and $(6.0 \pm 0.1) \times 10^{-8}$ m^2 s^{-1}, respectively, are much smaller than the values for heptane (8.01×10^{-8} m^2 s^{-1}) or ethanol (8.70×10^{-8} m^2 s^{-1}). Contrary to what is expected from these values of thermal diffusivity, the cooling rates observed in the ionic liquids are similar to that in ethanol and are larger than that in heptane (Figure 6). It seems that, for ionic liquids, thermal diffusivity does not represent the energy transfer process at the microscopic level.

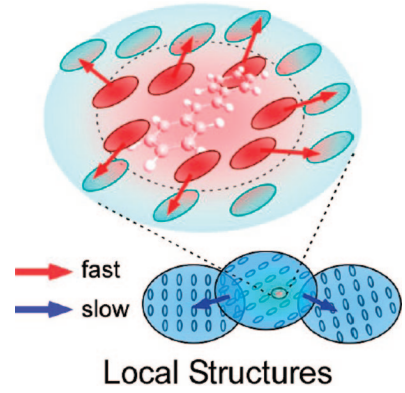

FIGURE 7. Model for the cooling process in ionic liquids.

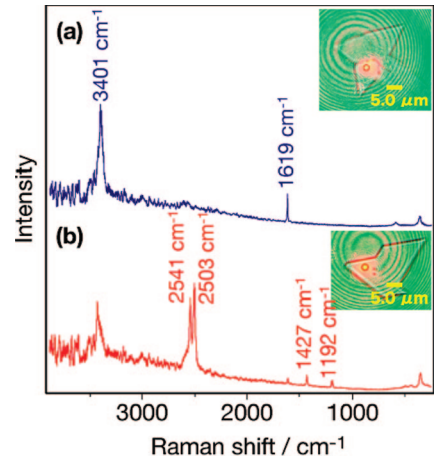

FIGURE 8. Raman spectra of crystals formed in $C_4mim[FeCl_4]$ (a) and $C_4mim[FeCl_4]$ treated with D_2O (b). The insets show the microscopic image of the measured crystals with the laser spot (circle) used for the Raman measurements.

The cooling rate of a solute may not show a good correlation with macroscopic thermal diffusivity of the solvent if there are local structures formed in the solvent, as we expect for C_2mimTf_2N and C_4mimTf_2N. The picosecond cooling process is determined by the energy transfer within a group of solvents that are surrounding the solute. By the time the flow of the excess energy of 3000 cm^{-1} reaches the boundary of the local structure, it is already distributed to the many degrees of freedom of a large number of solvent molecules. The temperature may well be cooled back to the room temperature at that time. The whole cooling process is thus completed within the local structure. The macroscopic heat conduction, however, proceeds over the boundary between the local structures. If the energy transfer between a pair of local structures is less effective than the energy transfer within the local structures, then macroscopic heat conduction is controlled by the inter-local-structure energy transfer as shown in Figure 7. We consider that the apparent discrepancy between the thermal diffusivity dependence of the cooling rate in the molecular liquids and that in the ionic liquids indicates the presence of local structures in C_2mimTf_2N and C_4mimTf_2N.

Extraordinary Nanoenvironments in a Magnetic Ionic Liquid, C_4mim[$FeCl_4$]

Local structures in imidazolium-based ionic liquids may well produce extraordinary molecular environments and hence lead to novel molecular phenomena that have not been found for molecular liquids. Here, we describe two newly found phenomena that are ascribable to such molecular environments in C_4mim[$FeCl_4$]. C_4mim[$FeCl_4$] is a prototype magnetic ionic liquid that shows strong response to a magnet.[52–54] Raman spectroscopy has indicated that the cation structure in C_4mim[$FeCl_4$] is very similar to those in the other $C_n$mim-based ionic liquids discussed in the preceding sections.[52]

In the course of Raman spectroscopic examination of liquid C_4mim[$FeCl_4$] under a microscope, we accidentally found that unknown crystals occasionally formed when the liquid was irradiated by the back illuminating light.[55] It was later confirmed that the crystal formation was accelerated by ultraviolet irradiation at 365 nm. We suspect that a photochemical reaction of the $FeCl_4^-$ anion results in this crystal formation (see discussion below). The Raman spectrum of one of those crystals is given in Figure 8a. As shown in the inset of the figure, the formed crystal has sharp edges characteristic of a single crystal. The Raman spectrum shows two prominent bands at 3401 and 1619 cm^{-1} and two weaker bands in the low-frequency region. This spectral pattern is quite different from those of C_4mim[$FeCl_4$]; neither the C_4mim^+ nor the $FeCl_4^-$ bands are observed. The frequencies 3401 and 1619 cm^{-1} happen to be close to those of water. We therefore repeated the same experiment under a D_2O atmosphere with an expectation that water impurity absorbed from the atmosphere might play a role.[56] The resultant Raman spectrum is shown in Figure 8b. A crystal similar to that in spectrum a was obtained. In spectrum b, in addition to the two peaks observed also in spectrum a, four peaks are observed at 2541, 2503, 1427, and 1192 cm^{-1}. These spectral changes are consistent with the assignments of the two prominent bands in spectrum a to water, 3401 cm^{-1} (symmetric OH stretch) and 1619 cm^{-1}(HOH bend). The new bands observed in spectrum b are assigned accordingly: 2541 cm^{-1} (OD stretch of HDO), 2503 cm^{-1} (symmetric OD stretch of D_2O), 1427 cm^{-1} (HOD bend), and 1192 cm^{-1} (DOD bend). The spectral change in the low frequency region can be ascribed to lattice vibrations including water molecules.

It is obvious that water molecules are contained with an extremely high concentration in the crystal formed in C_4mim[$FeCl_4$]. It is also clear that all the observed water bands show much smaller widths than those in ice and liquid water. In particular, the full width at half-maximum (fwhm) of the HOH bend band in the spectrum a is less than 9 cm^{-1}. As far as the authors are aware, such a sharp HOH band of water has never been reported. These unusually sharp bands are indicative of unusual structure of water molecules in the crystal. If the crystal contains water molecules only, it is a new form of ice at room temperature. We note this tempting possibility. We also note the possibility that some unknown species, which is silent in Raman spectroscopy, is contained in the crystal. For example, a clathrate hydrate structure, $(H_2O)_nHCl$, in which a chloride anion is loosely bound in a water cage $(H_2O)_nH^+$, is conceivable. Under UV irradiation, the $FeCl_4^-$ anion can be photohydrated to $FeCl_3(OH)^-$ and generate H^+ and Cl^-. Then, the H^+ and Cl^- ions are likely to be present in the irradiated ionic liquid and play a role in the crystal formation.

Separation of the crystals formed in C_4mim[$FeCl_4$] has so far been unsuccessful, hindering its X-ray structural analysis. Whatever the chemical composition might be, the uniqueness of the crystal must be a reflection of extraordinary molecular environments specific to C_4mim[$FeCl_4$]. The relevance of magnetic interactions with this crystal formation is not clear yet.

The other new phenomenon is the magnetic-field-dependent fabrication of nanostructures of conducting polymers in C_4mim[$FeCl_4$]. We found that nanoparticles and rod-like structures of conducting polymers (polypyrrole, *N*-methyl-polypyrrole, polythiophene) formed by simply adding monomer liquids to C_4mim[$FeCl_4$].[57] It was also found that the formed nanostructures were dependent on the external magnetic field. Figure 9 shows the SEM (scanning electron microscope) images of polypyrrole synthesized by this method with and without an external magnetic field. Without an external magnetic field (Figure 9a), nanoscale particles with 60 ± 20 nm diameter were formed (see also inset a-1). With an external magnetic field (Figure 9b), the particles tend to be aligned in a particular direction and a rod-like structure is formed. It is highly

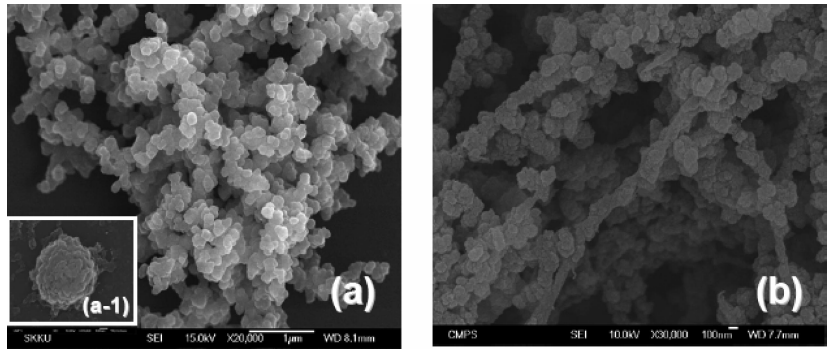

FIGURE 9. SEM images of the nanostructures of polypyrrole formed in C_4mim[$FeCl_4$] without (a) and with (b) an external magnetic field (1.3 T).

likely that local structures in C_4mim[$FeCl_4$] give rise to specific nanoenvironments that cause the formation of nanostructures and that these local structures and hence the nanoenvironments can be regulated by an external magnetic field. Nanostructure formation in nonmagnetic ionic liquids has been reported.[58,59]

Conclusion

It seems beyond doubt that specific local structures are formed in imidazolium-based ionic liquids. The next step is to characterize these local structures and clarify the structure–property and structure–function relationships in these ionic liquids. Coexistence of local structures with different size can make the free-energy landscape extremely complicated with a large number of shallow local minima.[1] An ionic liquid system may have an unusually long thermal relaxation time on account of this complicated energy landscape. We cannot rule out the possibility that it is even longer than our lifetime! New physicochemical approaches and standpoints, both experimental and theoretical, must be taken in order to correctly address this problem. Elucidation of local structures in ionic liquids may alter the concept of thermal equilibrium and the definition of material phase based on it.

The authors are grateful to all the coauthors of the papers that have founded the discussion presented in this Account.

Note Added after ASAP Publication: This manuscript was released ASAP on October 27, 2007 with an incorrect version of Figure 4. The correct version was posted on November 20, 2007.

References

(1) Hamaguchi, H.; Ozawa, R. Structure of Ionic Liquids and Ionic Liquid Compounds: Are Ionic Liquids Genuine Liquids in the Conventional Sense? *Adv. Chem. Phys.* **2005**, *131*, 85–104.
(2) Ozawa, R.; Hayashi, S.; Saha, S.; Kobayashi, A.; Hamaguchi, H. Rotational Isomerism and Structure of the 1-Buthyl-3-methylimidazolium Cation in the Ionic Liquid State. *Chem. Lett.* **2003**, *32*, 948–949.
(3) Holbrey, J. D.; Reichert, W. M.; Nieuwenhuyzen, M.; Johnson, S.; Seddon, K. R.; Rogers, R. D. Crystal Polymorphism in 1-Butyl-3-methylimidazolium Halides: Supporting Ionic Liquid Formation by Inhibition of Crystallization. *Chem. Commun.* **2003**, 1636–1637.
(4) Saha, S.; Hayashi, S.; Kobayashi, A.; Hamaguchi, H. Crystal Structure of 1-Butyl-3-methylimidazolium Chloride. A Clue to the Elucidation of the Ionic Liquid Structure. *Chem. Lett.* **2003**, *32*, 740–741.
(5) Hayashi, S.; Ozawa, R.; Hamaguchi, H. Raman Spectra, Crystal Polymorphism, and Structure of a Prototype Ionic liquid [bmim]Cl. *Chem. Lett.* **2003**, *32*, 498–499.
(6) Shepard, N.; Szasz, G. J. Spectroscopic Studies of Rotational Isomerism. III. The Normal Paraffins in the Liquid and Solid States. *J. Chem. Phys.* **1949**, *17*, 86–92.
(7) Snyder, R. G. Vibrational Study of the Chain Conformation of the Liquid *n*-Paraffins and Molten Polyethylene. *J. Chem. Phys.* **1967**, *47*, 1316–1360.
(8) Katayanagi, H.; Hayashi, S.; Hamaguchi, H.; Nishikawa, K. Structure of an Ionic Liquid, 1-*n*-Butyl-3-methylimidazolium Iodide, Studied by Wide-Angle X-ray Scattering and Raman Spectroscopy. *Chem. Phys. Lett.* **2004**, *392*, 460–464.
(9) Dupont, J. On The Solid, Liquid and Solution Structural Organization of Imidazolium Ionic Liquids. *J. Braz. Chem. Soc.* **2004**, *15*, 341–350.
(10) Triolo, A.; Russina, O.; Bleif, H.-J.; Di Cola, E. Nanoscale Segregation in Room Temperature Ionic Liquids. *J. Phys.Chem. B* **2007**, *111*, 4641–4644.
(11) Schröder, U.; Wadhawan, J. D.; Compton, R. G.; Marken, F.; Suarez, P. A. Z.; Consorti, C. S.; de Souza, R. F.; Dupont, J. Water-Induced Accelerated Ion Diffusion: Voltammetric Studies in 1-Methyl-3-[2,6-(*S*)-dimethylocten-2-yl]imidazolium Tetrafluoroborate, 1-Butyl-3-Methylimidazolium Tetrafluoroborate and Hexafluorophosphate Ionic Liquids. *New J. Chem.* **2000**, *24*, 1009–1015.
(12) Tokuda, H.; Hayamizu, K.; Ishii, K.; Susan, M. A. B. H.; Watanabe, M. Physicochemical Properties and Structures of Room Temperature Ionic Liquids. 1. Variation of Anionic Species. *J. Phys. Chem. B* **2004**, *108*, 16593–16600.
(13) Hardacre, C.; Holbrey, J. D.; McMath, S. E. J.; Bowron, D. T.; Soper, A. K. Structure of Molten 1,3-Dimethylimidazolium Chloride Using Neutron Diffraction. *J. Chem. Phys.* **2003**, *118*, 273–278.
(14) Gordon, C. M.; McLean, A. J. Photoelectron Transfer from Excited-State Ruthenium(II) Tris(bipyridyl) to Methylviologen in an Ionic Liquid. *Chem. Commun.* **2000**, 1395–1396.
(15) Ozawa, R.; Hamaguchi, H. Does Photoisomerization Proceed in an Ionic Liquid? *Chem. Lett.* **2001**, 736–737.
(16) Skrzypczak, A.; Neta, P. Diffusion-controlled electron-transfer reactions in ionic liquids. *J. Phys. Chem. A* **2003**, *107*, 7800–7803.
(17) Mandal, P. K.; Sarkar, M.; Samanta, A. Excitation-Wavelength-Dependent Fluorescence Behavior of Some Dipolar Molecules in Room-Temperature Ionic Liquids. *J. Phys. Chem. A* **2004**, *108*, 9048–9053.
(18) Iwata, K.; Kakita, M.; Hamaguchi, H. Picosecond Time-Resolved Fluorescence Study on Solute–Solvent Interaction of 2-Aminoquinoline in Room-Temperature Ionic Liquids: π–π Aromatic Complex Formation and Unusually Slow Rotational Diffusion. *J. Phys. Chem. B* **2007**, *111*, 4914–4919.
(19) Popolo, M. G. D.; Voth, G. A. On The Structure and Dynamics of Ionic Liquids. *J. Phys. Chem. B* **2004**, *108*, 1744–1752.
(20) Lopes, J. N. A C.; Pádua, A. A. H. Nanostructural Organization in Ionic Liquids. *J. Phys. Chem. B* **2006**, *110*, 3330–3335.
(21) Wang, Y.; Voth, G. Tail Aggregation and Domain Diffusion in Ionic Liquids. *J. Phys. Chem. B* **2006**, *110*, 18601–18608.
(22) Hu, Z.; Margulis, C. J. Heterogeneity in a Room-Temperature Ionic Liquid: Persistent Local Environments and the Red-Edge Effect. *Proc. Natl. Acad. Sci. U.S.A.* **2006**, *103*, 831–836.
(23) James, D. W. Low Frequency Depolarized Light Scattering from Liquids and Solutions. *Adv. Infrared Raman Spectrosc.* **1985**, *12*, 311–340.
(24) Faurskov-Nielsen, O. Low-Frequency Spectroscopic Studies of Interactions in Liquids. *Annu. Rep. Prog. Chem., Sect. C* **1993**, *90*, 3–44.
(25) Hyun, B. R.; Dzyuba, S. V.; Bartsch, R. A.; Quitevis, E. L. Intermolecular Dynamics of Room-Temperature Ionic Liquids: Femtosecond Optical Kerr Effect Measurements on 1-Alkyl-3-methylimidazolium Bis((trifluoromethyl)sulfonyl)imides. *J. Phys. Chem. A* **2002**, *106*, 7579–7585.
(26) Giraud, G.; Gordon, C. M.; Dunkin, I. R.; Wynne, K. The Effects of Anion and Cation Substitution on the Ultrafast Solvent Dynamics of Ionic Liquids: A Time-Resolved Optical Kerr-Effect Spectroscopic Study. *J. Chem. Phys.* **2003**, *119*, 464–477.
(27) Cang, H.; Li, J.; Fayer, M. D. Orientational Dynamics of The Ionic Organic Liquid 1-Ethyl-3-Methylimidazolium Nitrate. *J. Chem. Phys.* **2003**, *119*, 13017–13023.
(28) Shirota, H.; Castner, E. W. Why Are Viscosities Lower for Ionic Liquids with–$CH_2Si(CH_3)_3$ vs–$CH_2C(CH_3)_3$ Substitutions on the Imidazolium Cations? *J. Phys. Chem. B* **2005**, *109*, 21576–21585.
(29) Li, J.; Wang, I.; Fruchey, K.; Fayer, M. D. Dynamics in Supercooled Ionic Organic Liquids and Mode Coupling Theory Analysis. *J. Phys. Chem. A* **2006**, *110*, 10384–10391.
(30) Xiao, D.; Rajian, J. R.; Li, S. F.; Bartsch, R. A.; Quitevis, E. L. Additivity in the Optical Kerr Effect Spectra of Binary Ionic Liquid Mixtures: Implications for Nanostructural Organization. *J. Phys. Chem. B* **2006**, *110*, 16174–16178.
(31) Xiao, D.; Rajian, J. R.; Cady, A.; Li, S.; Bartsch, R. A.; Quitevis, E. L. Nanostructural Organization and Anion Effects on the Temperature Dependence of the Optical Kerr Effect Spectra of Ionic Liquids. *J. Phys. Chem. B* **2007**, *111*, 4669–4677.
(32) Shirota, H.; Wishart, J. F.; Castner, E. W. Intermolecular Interactions and Dynamics of Room Temperature Ionic Liquids That Have Silyl- and Siloxy-Substituted Imidazolium Cations. *J. Phys. Chem. B* **2007**, *111*, 4819–4829.
(33) Asaki, M. L. T.; Redondo, A.; Zawodziski, T. A.; Taylor, A. J. Dielectric Relaxation and Underlying Dynamics of Acetonitrile and 1-Ethyl-3-Methylimidazolium Triflate Mixtures Using THz Transmission Spectroscopy. *J. Chem. Phys.* **2002**, *116*, 10377–10385.
(34) Yamamoto, K.; Tani, M.; Hangyo, M. Terahertz Time-Domain Spectroscopy of Imidazolium Ionic Liquids. *J. Phys. Chem. B* **2007**, *111*, 4854–4859.
(35) Shuker, R.; Gammon, R. W. Raman-Scattering Selection-Rule Breaking and the Density of States in Amorphous Materials. *Phys. Rev. Lett.* **1970**, *25*, 222–225.

(36) Frisch, M. J.; Trucks, G. W.; Schlegel, H. B.; Scuseria, G. E.; Robb, M. A.; Cheeseman, J. R.; Montgomery, J. A., Jr.; Vreven, T.; Kudin, K. N.; Burant, J. C.; Millam, J. M.; Iyengar, S. S.; Tomasi, J.; Barone, V.; Mennucci, B.; Cossi, M.; Scalmani, G.; Rega, N.; Petersson, G. A.; Nakatsuji, H.; Hada, M.; Ehara, M.; Toyota, K.; Fukuda, R.; Hasegawa, J.; Ishida, M.; Nakajima, T.; Honda, Y.; Kitao, O.; Nakai, H.; Klene, M.; Li, X.; Knox, J. E.; Hratchian, H. P.; Cross, J. B.; Bakken, V.; Adamo, C.; Jaramillo, J.; Gomperts, R.; Stratmann, R. E.; Yazyev, O.; Austin, A. J.; Cammi, R.; Pomelli, C.; Ochterski, J. W.; Ayala, P. Y.; Morokuma, K.; Voth, G. A.; Salvador, P.; Dannenberg, J. J.; Zakrzewski, V. G.; Dapprich, S.; Daniels, A. D.; Strain, M. C.; Farkas, O.; Malick, D. K.; Rabuck, A. D.; Raghavachari, K.; Foresman, J. B.; Ortiz, J. V.; Cui, Q.; Baboul, A. G.; Clifford, S.; Cioslowski, J.; Stefanov, B. B.; Liu, G.; Liashenko, A.; Piskorz, P.; Komaromi, I.; Martin, R. L.; Fox, D. J.; Keith, T.; Al-Laham, M. A.; Peng, C. Y.; Nanayakkara, A.; Challacombe, M.; Gill, P. M. W.; Johnson, B.; Chen, W.; Wong, M. W.; Gonzalez, C.; Pople, J. A. *Gaussian 03*, revision C.02, Gaussian, Inc., Wallingford, CT, 2004.

(37) Mizushima, S.; Shimanouchi, T. Raman Frequencies of *n*-Paraffin Molecules. *J. Am. Chem. Soc.* **1949**, *71*, 1320–1324.

(38) Shigeto, S.; Hamaguchi, H. A new nonlinear Raman probe for local structures in liquids and solutions. *Chem. Phys. Lett.* **2006**, *417*, 149–153.

(39) Shigeto, S.; Hamaguchi, H. Evidence for mesoscopic local structures in ionic liquids: CARS signal spatial distribution of C(*n*) mim[PF_6] (*n*=4,6,8). *Chem. Phys. Lett.* **2006**, *427*, 329–332.

(40) Ishibashi, T.; Hamaguchi, H. Partially Coherent Anti-stokes Raman Scattering (PCARS). *Chem. Phys. Lett.* **1990**, *175*, 543–547.

(41) Ishibashi, T.; Hamaguchi, H. Comparative Study of Partially Coherent Anti-Stokes Raman Scattering (PCARS) and Rayleigh Scattering - Concentration and Temperature Dependence of Scattered Intensities. *J. Chem. Phys.* **1997**, *106*, 11–17.

(42) Huddleston, J. G.; Visser, A. E.; Reichert, W. M.; Willauer, G. A.; Broker, G. A.; Rogers, R. D. Characterization and Comparison of Hydrophilic and Hydrophobic Room Temperature Ionic Liquids Incorporating The Imidazolium Cation. *Green Chem.* **2001**, *3*, 156–164.

(43) Laubereau, A.; Kaiser, W. Vibrational Dynamics of Liquids and Solids Investigated by Picosecond Light Pulses. *Rev. Mod. Phys.* **1978**, *50*, 607–665.

(44) Iwata, K.; Yamaguchi, S.; Hamaguchi, H. Construction of a Transform-Limited Picosecond Time-Resolved Raman Spectrometer. *Rev. Sci. Instrum.* **1993**, *64*, 2140–2146.

(45) Hamaguchi, H.; Gustafson, T. L. Ultrafast Time-Resolved Spontaneous and Coherent Raman Spectroscopy: The Structure and Dynamics of Photogenerated Transient Species. *Annu. Rev. Phys. Chem.* **1994**, *45*, 593–622.

(46) Weaver, W. L.; Huston, L. A.; Iwata, K.; Gustafson, T. L. Solvent/Solute Interactions Probed by Picosecond Transient Raman Spectroscopy: Mode Specific Vibrational Dynamics in S_1*trans*-Stilbene. *J. Phys. Chem.* **1992**, *96*, 8956–8961.

(47) Iwata, K.; Hamaguchi, H. Picosecond Structural Relaxation of S_1*trans*-Stilbene in Solution as Revealed by Time-Resolved Raman Spectroscopy. *Chem. Phys. Lett.* **1992**, *196*, 462–468.

(48) Hamaguchi, H.; Iwata, K. Physical Chemistry of S_1*trans*-Stilbene in Solution as Studied by Time-Resolved Raman Spectroscopy. *Bull. Chem. Soc. Jpn.* **2002**, *75*, 883–897.

(49) Iwata, K.; Hamaguchi, H. Microscopic Mechanism of the Solute–Solvent Energy Dissipation Probed by Picosecond Time-Resolved Raman Spectroscopy. *J. Phys. Chem. A* **1997**, *101*, 632–637.

(50) Iwata, K.; Yoshida, K.; Takada, Y.; Hamaguchi, H. Vibrational Cooling Process of S_1*trans*-Stilbene in Ionic Liquids Observed with Picosecond Time-Resolved Raman Spectroscopy. *Chem. Lett.* **2007**, *36*, 504–505.

(51) Frez, C.; Diebold, G. J.; Tran, C. D.; Yu, S. Determination of Thermal Diffusivities, Thermal Conductivities, and Sound Speeds of Room-Temperature Ionic Liquids by the Transient Grating Technique. *J. Chem. Eng. Data* **2006**, *51*, 1250–1255.

(52) Hayashi, S.; Hamaguchi, H. Discovery of a Magnetic Ionic Liquid [bmim]$FeCl_4$. *Chem. Lett.* **2004**, *33*, 1590–1591.

(53) Okuno, M.; Hayashi, S.; Hamaguchi, H. Magnetic Manipulation of Materials in a Magnetic Ionic Liquid. *Appl. Phys. Lett.* **2006**, *89*, 132506.

(54) Hayashi, S.; Saha, S.; Hamaguchi, H. A New Class of Magnetic Fluids: bmim[$FeCl_4$] and nbmim[$FeCl_4$] Ionic Liquids. *IEEE Trans. Magn.* **2006**, *42*, 12–14.

(55) Miki, H.; Hayashi, S.; Kikura, H.; Hamaguchi, H. Raman Spectra Indicative of Unusual Water Structure in Crystals Formed from a Room-Temperature Ionic Liquid. *J. Raman Spectrosc.* **2006**, *37*, 1242–1243.

(56) Saha, S.; Hamaguchi, H. Effect of Water on the Molecular Structure and Arrangement of Nitrile-Functionalized Ionic Liquids. *J. Phys. Chem. B* **2006**, *110*, 2777–2781.

(57) Kim, J. Y.; Kim, J. T.; Min, Y. K.; Hamaguchi, H. *Macromolecules*,submitted.

(58) Antonietti, M.; Kuang, D.; Smarsly, B.; Zhou, Y. Ionic Liquids for the Convenient Synthesis of Functional Nanoparticles and Other Inorganic Nanostructures. *Angew. Chem., Int. Ed.* **2004**, *43*, 4988–4992.

(59) Itoh, H.; Naka, K.; Chujo, Y. Synthesis of Gold Nanoparticles Modified with Ionic Liquid Based on the Imidazolium Cation. *J. Am. Chem. Soc.* **2004**, *126*, 3026–3027.

AR700074C